JOURNAL OF GUIDANCE, CONTROL, AND DYNAMICS
Vol. 15, No. 5, September-October 1992

Robust Control for a Noncollocated Spring-Mass System

Richard Braatz* and Manfred Morari†
California Institute of Technology, Pasadena, California 91125

Robust control laws are presented for an undamped pair of coupled masses with a noncollocated sensor and actuator. This simple problem captures many of the features of more complex aircraft and space structure vibration control problems. The control problem is formulated in the structured singular value framework, which addresses the stability robustness to parameter variations directly. Controllers are designed by D-K iteration (commonly called μ synthesis), and the resulting high-order controllers are reduced using Hankel model reduction. Design specifications such as settling time, actuator constraints, insensitivity to measurement noise, and parameter uncertainty are achieved by the resulting controllers.

I. Introduction

THE objective of this paper is to describe control system design for a coupled spring-mass system. This simple control problem was formulated to capture many of the features of more complex aircraft and space structure control problems. The designed controllers must be robust to parametric uncertainty in the two masses and the spring constant and must meet specifications such as settling time, actuator constraints, and insensitivity to measurement noise. The problem was formulated in Ref. 1 as a benchmark control problem, to which numerous researchers have applied a variety of robust control design methodologies (as listed in Ref. 2).

In Ref. 3, solutions to the benchmark control problem presented at the 1990 American Control Conference were tested in terms of their settling time, maximum actuator movement, and robustness to parametric uncertainty. The settling time and robustness specifications came from the benchmark problem statement in Ref. 1. For comparison in Ref. 3, the peak actuator use was limited to one.

It was found that 2 out of 10 controllers achieved the desired 15-s settling time, 4 controllers exceeded the actuator constraint, and 4 control designs did not meet the robustness specification. None of the controllers met all of the specifications of the design problem. Many of the controllers had an infinite bandwidth, which in practice would amplify high-frequency measurement noise.

This paper shows how to address the specifications within the structured singular value framework. Although the design specifications cannot be described directly in the structured singular value framework, this paper will show how to choose with little effort the control, performance, disturbance, and measurement weights necessary to meet the design specifications.

The paper is organized as follows. In Sec. II, the benchmark problem is briefly described and two sets of design specifications are given. The structured singular value framework is briefly reviewed in Sec. III. In Sec. IV, controllers are designed that meet the specifications in Sec. II. The control designs are discussed in Sec. V. Conclusions are given in Sec. VI.

II. Benchmark Problem

The benchmark problem is described in Ref. 2 and thus will not be described in detail here.

Consider the two-mass/spring system in Ref. 2, which is a generic model of an uncertain dynamic system with a noncollocated sensor and actuator. The system is represented in state-space form as

$$\dot{x} = \begin{bmatrix} \dot{x}_1 \\ \dot{x}_2 \\ \dot{x}_3 \\ \dot{x}_4 \end{bmatrix} = \begin{bmatrix} 0 & 0 & 1 & 0 \\ 0 & 0 & 0 & 1 \\ -k/m_1 & k/m_1 & 0 & 0 \\ k/m_2 & -k/m_2 & 0 & 0 \end{bmatrix} \begin{bmatrix} x_1 \\ x_2 \\ x_3 \\ x_4 \end{bmatrix} + \begin{bmatrix} 0 \\ 0 \\ 1/m_1 \\ 0 \end{bmatrix} u + \begin{bmatrix} 0 \\ 0 \\ 0 \\ 1/m_2 \end{bmatrix} w \tag{1}$$

$$y = x_2 + v \tag{2}$$

$$z = x_2 \tag{3}$$

where x_1 and x_2 are the positions of body 1 and body 2, respectively; x_3 and x_4 are the velocities of body 1 and body 2, respectively; u is the control input acting on body 1; y is the sensor measurement; w is the disturbance acting on body 2; v is sensor noise; z is the output to be controlled; k is the spring constant; m_1 is the mass of body 1; and m_2 is the mass of body 2.

The coupled spring-mass system is assumed to have negligible damping. The spring constant and masses are assumed to be uncertain. The actuator is located on body 1, and the sensor is located on body 2; i.e., the sensor and actuator are noncollocated. This makes the system much harder to control than in the collocated case.

Certain control specifications of the benchmark problem described in Ref. 2 are given concretely, whereas other specifications were left to the control designer. We adopt the exact specifications regarding the nominal settling time and robustness to parametric uncertainty from Ref. 2. We choose the measurement noise to be approximately the same as that for the laboratory flexible structure in Ref. 4. The actuator constraint is that of Ref. 3. Our actuator bandwidth limitation is more restrictive than that for the voice coil actuators in Ref. 4. The two design problems are defined in the following.

Design 1. Design a compensator with the following properties:

1) The closed-loop system is stable for $m_1 = m_2 = 1$ and $0.5 \le k \le 2.0$.

2) For $w(t) =$ unit impulse at $t = 0$, the performance variable z has a settling time of 15 s for the nominal system $m_1 = m_2 = k = 1$. The settling time is defined to be the time re-

Received Sept. 4, 1991; revision received Nov. 3, 1991; accepted for publication Dec. 17, 1991.

*Graduate Student, Department of Chemical Engineering.
†McCollum-Corcoran Professor, Department of Chemical Engineering.

quired for the output to reach and stay within 10% of its peak value.

3) The control system can tolerate Gaussian white noise with variance of $9*10^{-6}$.

4) Because of finite actuator response time, the controller bandwidth must be ≤ 50 rad/s.

5) The control input $u(t)$ is limited to $|u| \leq 1$.

6) The number of controller states should be ≤ 4.

Design 2. Same as design 1 but replace property 1 with the following:

1′) Maximize the stability margin with respect to the three uncertain parameters m_1, m_2, k whose nominal values are $m_1 = m_2 = k = 1$.

III. Structured Singular Value Framework

The goal of any controller design is to ensure that the overall system is stable and satisfies some minimum performance requirements. These requirements should be satisfied at least when the controller is applied to the nominal plant; that is, nominal stability and nominal performance are required.

In practice the real plant G_p is not equal to the model G. The term "robust" is used to indicate that some property holds for a set Π of possible plants G_p as defined by the uncertainty description. In particular, by "robust stability" we mean that the closed-loop system is stable for all $G_p \in \Pi$. By "robust performance" we mean that the performance requirements are satisfied for all $G_p \in \Pi$. Performance is commonly defined in robust control theory using the H_∞ norm of some transfer function $\Sigma(G)$ of interest.

Definition 1. The closed-loop system exhibits nominal performance if

$$\|\Sigma\|_\infty \equiv \sup_\omega \bar{\sigma}(\Sigma) \leq 1 \tag{4}$$

Definition 2. The closed-loop system exhibits robust performance if

$$\|\Sigma_p\|_\infty \equiv \sup_\omega \bar{\sigma}(\Sigma_p) \leq 1, \qquad \forall G_p \in \Pi \tag{5}$$

For example, for rejection of disturbances at the plant output, Σ would be the weighted sensitivity:

$$\Sigma = W_1 S W_2, \qquad S = (I + GK)^{-1}$$
$$\Sigma_p = W_1 S_p W_2, \qquad S_p = (I + G_p K)^{-1} \tag{6}$$

In this case the input weight W_2 is usually chosen equal to the disturbance model. The output weight W_1 is used to specify the frequency range over which the sensitivity function should be small and to weight each output according to its importance, and K is the transfer function of the controller.

Doyle[5] derived the structured singular value μ to test for robust performance. To use μ we must model the uncertainty (the set Π of possible plants G_p) as norm bounded perturbations (Δ_i) on the nominal system. Through weights each perturbation is normalized to be of size one:

$$\bar{\sigma}(\Delta_i) \leq 1, \qquad \forall \omega \tag{7}$$

The perturbations, which may occur at different locations in the system, are collected in the diagonal matrix Δ_U (the U denotes uncertainty):

$$\Delta_U = \text{diag}[\Delta_1, \ldots, \Delta_n] \tag{8}$$

and the system is arranged to match the block diagrams in Fig. 1. The interconnection matrix M in Fig. 1 is determined by the nominal model (G), the size and nature of the uncertainty, the performance specifications, and the controller (K). The quantity μ is defined in the following.

Definition 3. Let M be a square complex matrix and define the set Δ as follows:

$$\Delta = \{\text{diag}[\Delta_1, \ldots, \Delta_n]\} \tag{9}$$

Then $\mu_\Delta(M)$ is defined such that $\mu_\Delta^{-1}(M)$ is equal to the smallest $\bar{\sigma}(\Delta)$ for Δ making $(I + \Delta M)$ singular, i.e.,

$$\mu_\Delta^{-1}(M) = \min_{\Delta \in \Delta} \{\bar{\sigma}(\Delta) : \det(I + \Delta M) = 0\} \tag{10}$$

For Fig. 1 robust stability can be tested by the following theorem:

Theorem 1. The closed-loop system exhibits robust stability if and only if the closed-loop system is nominally stable and

$$\sup_\omega \mu_{\Delta_U}(M_{11}) < 1 \tag{11}$$

The robust performance [Eq. (5)] can be tested by the following theorem.

Theorem 2. The closed-loop system exhibits robust performance if and only if the closed-loop system is nominally stable and

$$\sup_\omega \mu_\Delta(M) < 1 \tag{12}$$

The value of $\mu_\Delta(M)$ depends on both the elements of the matrix M and the structure of the perturbation matrix $\Delta = \text{diag}[\Delta_U, \Delta_P]$. The performance block Δ_P is often chosen to be a full square matrix with a dimension equal to the number of outputs (the subscript P denotes performance). Note that the issue of robust stability is simply a special case of robust performance. Also note that robust performance implies robust stability, i.e.,

$$\sup_\omega \mu_\Delta(M) \geq \sup_\omega \mu_{\Delta_U}(M_{11})$$

It is a key idea that μ is a general analysis tool for determining robust performance. Any system with uncertainty adequately modeled as in Eq. (7) can be put into $M - \Delta$ form, and robust performance can be tested using Eq. (12). Standard programs calculate M and Δ (Ref. 6), given the transfer functions describing the system components and the location of the uncertainty blocks Δ_i.

Computation of μ for Complex Δ

The μ with complex Δ is commonly calculated through upper and lower bounds. First, define two subsets of $C^{n \times n}$:

$$Q = \{Q \in \Delta : Q^* Q = I_n\} \tag{13}$$

where Q^* is the conjugate transpose of Q, I_n is the $n \times n$ identity matrix, and

$$D = \{\text{diag}[d_i I_i] : \dim(I_i) = \dim(\Delta_i),\ d_i \text{ positive real scalar}\} \tag{14}$$

Then, as seen in Ref. 5,

$$\max_{Q \in Q} \rho(QM) \leq \mu_\Delta(M) \leq \inf_{D \in D} \bar{\sigma}(DMD^{-1}) \tag{15}$$

A result of Doyle[5] is that the lower bound,

$$\max_{Q \in Q} \rho(QM)$$

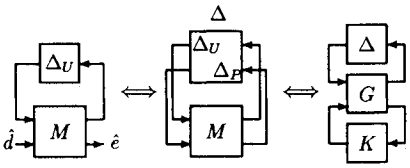

Fig. 1 General interconnection structures.

is always equal to $\mu_\Delta(M)$. Unfortunately, the maximization is not convex, and computing the global maximum of such functions is generally difficult. In contrast, the computation of the upper bound is convex. However, the upper bound is not necessarily equal to μ except when the number of complex Δ blocks is ≤ 3. The upper and lower bounds are almost always within a percent or so for real problems[7]; thus, for engineering purposes μ never has to be calculated exactly.

Controller Synthesis

M is a function of the controller K. The H_∞ optimal control problem is to find a stabilizing K that minimizes

$$\sup_\omega \bar{\sigma}\left[M(K)\right]$$

The state-space approach for solving the H_∞ control problem is described in Ref. 8.

The D-K iteration method (often called μ synthesis) is an ad hoc method that attempts to minimize the tight upper bound of μ in Eq. (15); i.e., it attempts to solve

$$\min_K \inf_{D \in D} \sup_\omega \bar{\sigma}\left[DM(K)D^{-1}\right] \tag{16}$$

The approach in D-K iteration is to alternatively minimize

$$\sup_\omega \bar{\sigma}\left[DM(K)D^{-1}\right]$$

for either K or D while holding the other constant. For fixed D the controller synthesis is solved via H_∞ optimization. For fixed K the quantity is minimized as a convex optimization. The resulting D as a function of frequency is fitted with an invertible stable minimum-phase transfer function and wrapped back into the nominal interconnection structure. This increases the number of states of the scaled G, which leads the next H_∞ synthesis step to give a higher-order controller. The iterations stop after

$$\sup_\omega \bar{\sigma}\left[DM(K)D^{-1}\right]$$

is <1 or is no longer diminished. The resulting high-order controller is reduced using Hankel model reduction.[9] Although this method is not guaranteed to converge to a global minimum, it has been used extensively to design robust controllers and seems to work well.[10]

Computation of μ for Real Δ

Techniques for computing μ for real parameter perturbations are summarized in Ref. 11. For one real uncertain parameter a simple method of determining the stability robustness is to plot the eigenvalues in the complex plane as a function of the parameter being varied. The resulting plot resembles a typical root locus plot, but as a function of the uncertain parameter instead of the controller gain. The parameter range for stability can then be read directly from the plot.

A simple but slow method of determining stability robustness for multiple real parameter variations is to systematically test points in the parameter space about the nominal point. The stability at each point is determined by calculating the eigenvalues. For three uncertain parameters, as needed to determine the stability robustness in design 2, the stability robustness can be determined in a reasonable amount of time. For problems with a larger number of uncertain real parameters, faster methods[12-14] must be used.

IV. Designs

Building the Generalized Block Diagram

The spring constant and the two masses are assumed to be uncertain and are given by

$$\begin{aligned} k &= k_0 + w_k \delta_k \\ m_1 &= m_{10} + w_1 \delta_1 \\ m_2 &= m_{20} + w_2 \delta_2 \end{aligned} \tag{17}$$

where k_0, m_{10}, and m_{20} are the nominal values and the weights w_k, w_1, and w_2 are used to normalize the uncertainties δ_i so that $|\delta_i| \leq 1$. Simultaneous perturbations in the δ_i are allowed, as long as $|\delta_i| \leq 1$ for each uncertainty i.

Weighted versions of the noise, disturbance, control input, and performance variable are given by

$$\begin{aligned} v &= w_v v' \\ w &= w_w w' \\ u' &= w_u u \\ z' &= w_z z \end{aligned} \tag{18}$$

where in general the input weights w_v and w_w weight the frequencies to be rejected and determine the relative importance of the noise and disturbance. The w_z is the performance weight, and w_u is used to limit the magnitude of the control input.

The symbols k, m_1, and m_2 from Eq. (17) and w, v, z, and u from Eq. (19) are substituted into the state-space equations [Eqs. (1-3)] and written in block diagram form in Fig. 2. The block diagram has x, u, v', and w' as inputs and $\dot{x}$, u', z', and y as outputs.

By inspection, the block diagram in Fig. 2 is rearranged to form the block diagram in Fig. 3, where

$$N = \begin{bmatrix} 0 & 0 & 1 & 0 & 0 & 0 & 0 & 0 & 0 & 0 \\ 0 & 0 & 0 & 1 & 0 & 0 & 0 & 0 & 0 & 0 \\ -\frac{k}{m_1} & \frac{k}{m_1} & 0 & 0 & -\frac{1}{m_1} & \frac{1}{m_1} & 0 & 0 & 0 & \frac{1}{m_1} \\ \frac{k}{m_1} & -\frac{k}{m_1} & 0 & 0 & \frac{1}{m_2} & 0 & \frac{1}{m_2} & 0 & \frac{w_w}{m_2} & 0 \\ w_k & -w_k & 0 & 0 & 0 & 0 & 0 & 0 & 0 & 0 \\ \frac{kw_1}{m_1} & -\frac{kw_1}{m_1} & 0 & 0 & \frac{w_1}{m_1} & -\frac{w_1}{m_1} & 0 & 0 & 0 & -\frac{w_1}{m_1} \\ -\frac{kw_2}{m_1} & \frac{kw_2}{m_1} & 0 & 0 & -\frac{w_2}{m_2} & 0 & -\frac{w_2}{m_2} & 0 & -\frac{w_2 w_w}{m_2} & 0 \\ 0 & 0 & 0 & 0 & 0 & 0 & 0 & 0 & 0 & w_u \\ 0 & w_z & 0 & 0 & 0 & 0 & 0 & 0 & 0 & 0 \\ 0 & 1 & 0 & 0 & 0 & 0 & 0 & w_v & 0 & 0 \end{bmatrix} \tag{19}$$

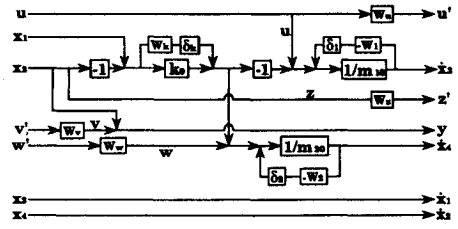

Fig. 2 Block diagram for coupled mass-spring system.

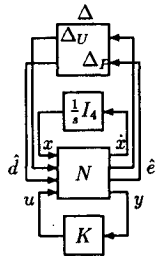

Fig. 3 Simplified block diagram for coupled mass-spring system.

and the normalized performance variable $\hat{e}$, the normalized disturbance $\hat{d}$, and the uncertainty block Δ_U are given by

$$\hat{e} = \begin{pmatrix} u' \\ z' \end{pmatrix} \tag{20}$$

$$\hat{d} = \begin{pmatrix} v' \\ w' \end{pmatrix} \tag{21}$$

$$\Delta_u = \begin{bmatrix} \delta_k & & \\ & \delta_1 & \\ & & \delta_2 \end{bmatrix} \tag{22}$$

The Δ_P is the performance Δ block, which relates the outputs to inputs, K is the controller transfer function, and I_4 is the 4×4 identity matrix. Closing the integrator loop in Fig. 3 gives the system interconnection structures in Fig. 1.

It can be seen from Eqs. (1-3) that the transfer function between the disturbance w and the output z contains a double integrator. In this case assumptions A1 and A3 in Ref. 8 needed to solve the H_∞ control problem are not satisfied. Ways of reformulating the problem to satisfy the assumptions are discussed in Refs. 8 and 15. It is suggested in Ref. 15 to either use a bilinear transform to move all open-loop poles off the imaginary axis, or to choose the disturbance and performance weights to cancel the integrators. Three methods are suggested in Ref. 8; the simplest method is to introduce an ϵ perturbation so that assumptions A1 and A3 are satisfied. Choosing this method, we slightly perturbed the poles on the imaginary axis by using $1/(s+0.00001)$ instead of $1/s$ in Fig. 3. However, all results reported here use the true integrator, and no problems were found to result from using the "almost-integrator" instead of the true integrator for the controller synthesis.

We will use the D-K iteration method by allowing the uncertainties in k, m_1, and m_2 to be complex. The D-K iteration method described in Sec. III approximately maximizes the performance for the worst-case plant described by the nominal plant plus the complex uncertainties. As such, the method will give a controller whose performance is insensitive to the complex uncertainties. Thus, the performance of the controller will also be insensitive to the corresponding real uncertainties.

Strategy for Choosing Input and Output Weights

The advantage of the structured singular value framework over many other design methods is that it yields directly controllers that are insensitive to model uncertainty. The disadvantage is that performance specifications such as 2 and 5 cannot explicitly be put in terms of the ∞ norm in Eq. (5). Although there is no explicit relationship between the performance specifications and the ∞ norm, decreasing the ∞ norm of the transfer function between the inputs w' and v' to the outputs z' and u' does improve the speed of response and decrease the peak outputs.

The key to the synthesis technique is the selection of the weights w_w, w_v, w_z, and w_u. The controller synthesis procedure is much faster when lower-order weights are used; thus, constant weights should be used when possible.

The approach to choosing the weights w_w, w_v, w_z, and w_u will be as follows. It can be shown that multiplying w_w and w_v by a scalar transfer function and dividing w_z and w_u by the same scalar transfer function does not change the ∞ norm in Eq. (5). Thus, without loss of generality we can take $w_w = 1$. Since the noise v is expected to have a much smaller effect on the system than the disturbance w, we will choose the noise weight w_v to be small. Noise weights typically are chosen to have larger gain at high frequency, but we expect that the effect of the noise on the system is small enough that choosing a frequency-dependent w_v will not give a controller much better than that when choosing a constant noise weight. If the simulations show sensitivity to measurement noise, then w_v will be increased.

There is no known explicit relationship between the frequency-dependent output weights w_z and w_u and the resulting settling time and peak control input. Some general empirical guidelines for choosing frequency-dependent weights include the following[16]:

1) Choose high gain weight at midrange to high frequency in order to give small peak values.

2) Choose an even higher gain at low frequency for good tracking.

Guideline 1 implies that w_u should have high gain at high frequencies to keep the peak control input small. High gain for w_u at high frequencies should also cause the controller to avoid high-frequency control inputs (specification 4).

It can be shown from Eqs. (1-3) that an impulse disturbance will give no steady-state offset in u and z as long as the controller is internally stable. Thus, w_u and w_z need not have a higher gain at low frequency (it is suspected that guideline 2 was intended only to be used to design for tracking of *step* inputs). Since high gain at low frequency is not needed for w_u and w_z, and low-order weights are desirable for controller synthesis, we will use constant w_u and w_z. Increasing w_u and w_z will increase the overall performance of u and z; this will decrease the peak control input and decrease the settling time, respectively. The w_u will be chosen to be large enough so that the peak control input constraint $\max_t |u(t)| \approx 1$ is met. The w_z will be chosen large enough so that the settling time specification 2 is met. If we could not achieve the design specifications using constant weights, then frequency-dependent weighting would be considered.

Defining μ for Robust Performance

Since the performance specifications are not explicitly in terms of the ∞ norm, we are not particularly interested in meeting condition (12). We are not interested in meeting condition (11) for robust stability for complex uncertainties, either. We are interested in meeting the stability robustness specification 1. In other words, the design is complete when specifications 1-4 are met, regardless of whether conditions (11) or (12) are satisfied.

The performance block Δ_P was chosen to be a diagonal matrix with two independent 1×1 blocks for all designs. This decouples the performance specifications that u be small (peak magnitude < 1) and that z respond quickly to a unit impulse in w. This makes choosing a satisfactory w_u and w_z easier. Also, μ for robust performance defined with this choice of Δ_P is less than μ for robust performance defined using the

typical choice of full block Δ_P. Thus, this choice for Δ_P gives a smaller difference between the structured singular value for robust performance and for robust stability, allowing the D-K iteration design method to more directly enhance stability robustness.

The specific control designs for the two sets of specifications follow.

Design 1

For the first design the mass uncertainty weights w_1 and w_2 are zero, i.e., $\Delta_U = \delta_k$. Since k is in the range $[k_{\min}, k_{\max}] = [0.5, 2.0]$, it is convenient to choose the nominal

$$k_0 = (k_{\max} + k_{\min})/2 = (2.0 + 0.5)/2 = 1.25$$

To normalize $|\delta_k| \le 1$, the uncertainty weight

$$w_k = (k_{\max} - k_{\min})/2 = 0.75$$

First, we choose only constant weights to specify w_w, w_v, w_z, and w_u. Without loss of generality we can choose one of these weights to be 1; we took $w_w = 1$. Since the measurement noise is small in magnitude compared to the size of the disturbance, we initially chose the noise weight to be much smaller than the disturbance weight, $w_v = w_w/100 = 0.01$. Increasing w_z decreases the peak value and settling time for z. Increasing w_u decreases the peak control input.

The D-K iteration design procedure was initially performed for $w_z = w_u = 1$. Simulations with the resulting controller showed that the nominal settling time specification was easily met, but the nominal peak control input was 11 and robust stability was not satisfied. To decrease the peak control input, w_u was increased to 15. Since robust stability was not satisfied and there was excess performance in z, we decided to trade off performance to get increased stability by decreasing w_z to 0.1. The design procedure was repeated with w_w and w_v unchanged. The resulting controller satisfied specifications 2–5, but again did not satisfy the robustness specification 1. The peak control input was ~ 1; thus, w_u was held constant. The settling time was ~ 10; thus, performance was again traded off with stability by decreasing w_z to 0.06. The design procedure was repeated to arrive at a design that meets all the design specifications 1–6. Each time the D-K iteration method was used, one D iteration was needed. Further D-K iterations did not diminish the objective in Eq. (16). The final 12-state controller was reduced to 4 states with negligible loss in stability and performance. The structured singular value for performance with the resulting controller is shown in Fig. 4.

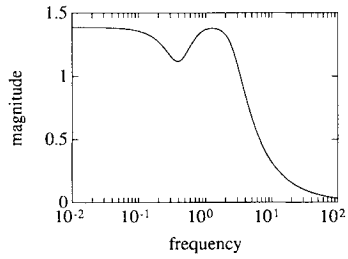

Fig. 4 Value of μ for robust performance: design 1.

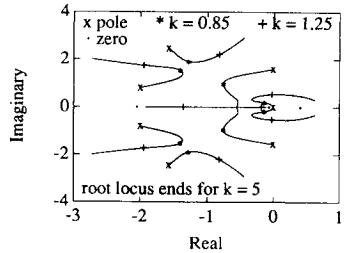

Fig. 5 Root locus: design 1.

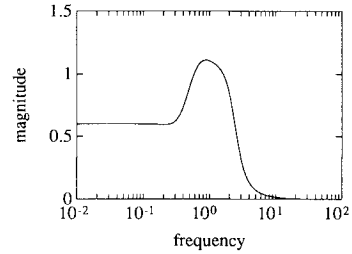

Fig. 6 Value of μ for complex robust stability: design 1.

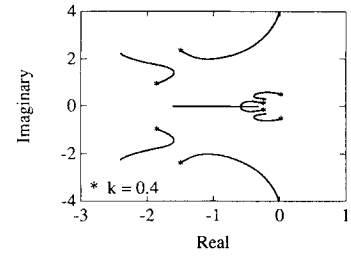

Fig. 7 Parameter root locus: design 1.

The controller after the Hankel model reduction has four states and is given by

$$A_c = \begin{bmatrix} -2.399 & -1.797 & 1.8066 & -3.025 \\ 3.744 & -0.7299 & -0.5626 & 2.258 \\ 0 & 0 & -1.717 & -1.116 \\ 0 & 0 & 0.6563 & -2.269 \end{bmatrix} \tag{23}$$

$$B_c = \begin{bmatrix} -3.705 \\ 0.6915 \\ 0.3345 \\ -2.784 \end{bmatrix} \tag{24}$$

$$C_c = \begin{bmatrix} 3.927 & -1.689 & -0.4837 & 1.885 \end{bmatrix} \tag{25}$$

$$D_c = 0.0008 \tag{26}$$

The zeros for the aforementioned controller are $\{27620, -2.088, -0.1061, 0.3712\}$, and the poles are $\{-1.564 \pm 2.456i, -1.993 \pm 0.8103i\}$. The zero at 27620 is so far in the right half plane that it has a negligible effect on stability and performance. This zero was dropped to make the final controller strictly proper. See Fig. 5 for the root locus for the final controller (the k in Fig. 5 refers to the root locus gain, not the spring constant).

The controller bandwidth (read from the controller's Bode magnitude plot) is 31 rad/s. The gain and phase margins are read from the Nyquist plot and found to be 1.25 and 19.7 deg, respectively. Figure 6 is a plot of the structured singular value for complex uncertainty. The μ for robust stability for complex uncertain k is read from the plot to be $\mu^c_{RS} = 1.11$. The parameter root locus as a function of the spring constant k is shown in Fig. 7. The root locus begins at $k = 0.4$ where two eigenvalues are in the right half plane. The unstable eigenvalues become stable for $k = 0.46$ and remain in the left half plane until $k = 6.8$. Thus, the closed-loop system is stable for $0.46 \le k \le 6.8$. Recalling that μ is the inverse of the smallest perturbation that destabilizes the system, we have that μ for real uncertainty is

$$\mu^r_{RS} = \frac{1}{\min\limits_{\delta_k \text{real}} \{|\delta_k| : \text{closed-loop system is unstable}\}} \tag{27}$$

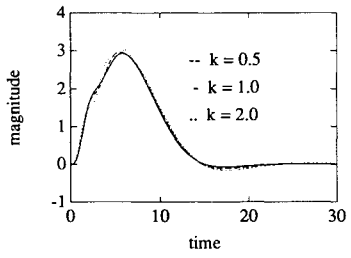

Fig. 8 Position of body 1, x_1: design 1.

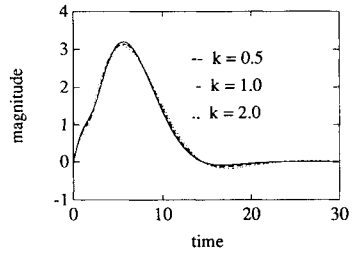

Fig. 9 Position of body 2, x_2: design 1.

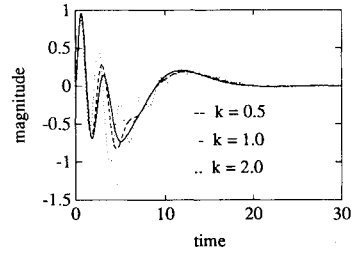

Fig. 10 Control input, u: design 1.

Substituting for δ_k from Eq. (17) gives

$$\mu_{RS}^r = \frac{1}{\min_k \{|(k-k_0)/w_k| : k \text{ destabilizing}\}} = \frac{1}{|(0.46-1.25)/0.75|} = 0.95 \tag{28}$$

The conservatism in using complex uncertain k over real uncertain k is

$$(\mu_{RS}^c - \mu_{RS}^r)/\mu_{RS}^r = (1.11-0.95)/0.95 = 17\%$$

The controller is robust to uncertainty in k while having small gain and phase margins. This indicates that the gain and phase margins are poor indicators of robustness, at least to parametric uncertainty in the spring constant k.

A unit impulse disturbance and Gaussian white noise with variance of $9*10^{-6}$ were used in all simulations. The time domain plots for the mass positions x_1 and x_2 and the control input u are given for $k = 0.5$, 1, and 2 (see Figs. 8–10). We see that all of the time responses are remarkably insensitive to uncertainty in k and to measurement noise. The settling time for both mass positions to a unit impulse disturbance for all $k \in [0.5,2]$ is 13 s. The maximum control input is <1. Frequency-dependent weights were not needed to meet all the specifications of design 1.

Design 2

The goal in this problem is to maximize the stability with respect to uncertain m_1, m_2, and k with nominal values $m_{10} = m_{20} = k_0 = 1$. Initially we designed for 20% complex uncertainty, i.e., $w_1 = w_2 = w_k = 0.2$. The initial input and output weights were chosen equal to those for the final design in design 1. The resulting controller met specifications 3–6. To meet the settling time specification 2, controller design procedure was repeated with the performance weight doubled to $w_z = 0.12$, with all other weights unchanged. The resulting controller met all the specifications 2–6. The settling time and peak control input were close to their maximum values; thus, performance could not be traded off for an appreciably larger stability margin (specification 1').

Each time the D-K iteration method was used, one D iteration was needed. Further D-K iterations did not diminish the objective in Eq. (16). The 24-state controller was reduced to 4 states with negligible loss in stability and performance. The structured singular value for performance with the resulting controller is in Fig. 11. The controller after the Hankel model reduction is given by

$$A_c = \begin{bmatrix} -0.5178 & -1.521 & -1.558 & -0.0820 \\ 4.725 & -5.510 & 5.878 & 0.4984 \\ 0 & 0 & -2.039 & 2.432 \\ 0 & 0 & -2.974 & -0.0832 \end{bmatrix} \tag{29}$$

$$B_c = \begin{bmatrix} -0.8847 \\ 2.702 \\ -3.259 \\ -0.8716 \end{bmatrix} \tag{30}$$

$$C_c = \begin{bmatrix} -1.471 & 4.125 & -0.5234 & -0.1214 \end{bmatrix} \tag{31}$$

$$D_c = 0.00372 \tag{32}$$

The zeros for the aforementioned controller are $\{-3847, -0.1392, 1.780 \pm 0.5621i\}$, and the poles are $\{-3.014 \pm 0.9775i, -1.061 \pm 2.505i\}$. The zero at -3847 is far in the left half plane and thus has a small effect on stability and performance. This zero was dropped to make the final controller strictly proper. See Fig. 12 for the root locus.

The controller bandwidth (read from the controller's Bode magnitude plot) is 21 rad/s. The gain and phase margins are read from the Nyquist plot and found to be 1.43 and 28.2 deg, respectively. Figure 13 is a plot of the structured singular value for robust stability with complex uncertainty. The peak value on this plot is $\mu_{RS}^c = 1.11$.

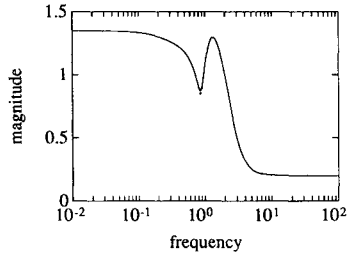

Fig. 11 Value of μ for robust performance: design 2.

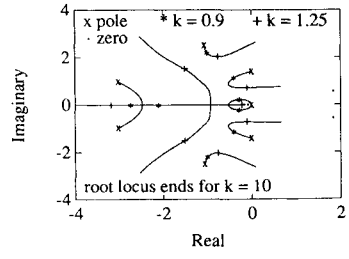

Fig. 12 Root locus: design 2.

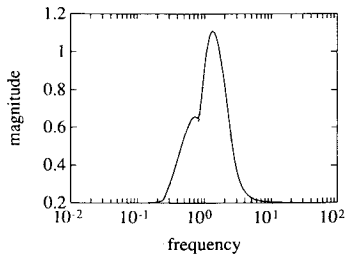

Fig. 13 Value of μ for complex robust stability: design 2.

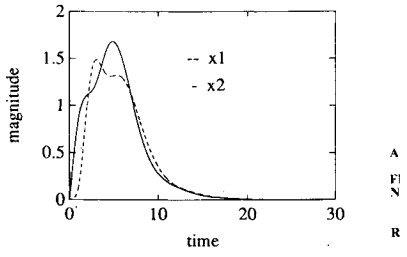

Fig. 14 Position of bodies 1 and 2: design 2.

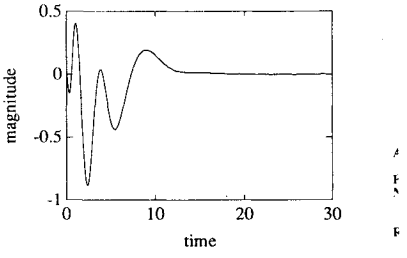

Fig. 15 Control input, u: design 2.

By use of the method described in Sec. III, the closed-loop system was found to be stable under simultaneous independent real parameter variations up to 30%; i.e., the closed-loop system is stable for any values of k, m_1, and m_2 given by

$$k \in [0.7,1.3], \qquad m_1 \in [0.7,1.3], \qquad m_2 \in [0.7,1.3] \tag{33}$$

Recalling that μ is the inverse of the smallest perturbation that destablizes the system, we have that μ for real uncertainty is

$$\mu^r_{RS} = \frac{1}{\min_{\gamma}\{\gamma : \delta_k \in [-\gamma,\gamma];\ \delta_1 \in [-\gamma,\gamma];\ \delta_2 \in [-\gamma,\gamma];\ \text{closed-loop system is unstable}\}} \tag{34}$$

Substituting δ_k, δ_1, and δ_1 from Eq. (17) and recalling that $w_1 = w_2 = w_k = 0.2$ gives $\mu^r_{RS} = 0.2/0.3 = 2/3$. The conservatism in using complex uncertainty in k, m_1, and m_2 over using real uncertainty is

$$(\mu^c_{RS} - \mu^r_{RS})/\mu^r_{RS} = (1.11 - 0.67)/0.67 = 67\%$$

The lower and upper parameter margins (with $m_1 = m_2 = 1$) for k are 0.55 and 2.5, respectively. The lower and upper parameter margins for m_1 (with $k = m_2 = 1$) are 0 and 3.4, respectively. The m_2 has the same parameter margins as those for m_1.

The time domain plots for the mass positions x_1 and x_2 and the control input u are given for $m_1 = m_2 = k = 1$ (see Figs. 14 and 15). The settling times for both x_1 and x_2 are < 15 s. The maximum control input is < 1. All responses are insensitive to measurement noise. All specifications of design 2 are met.

V. Discussion

The gain and phase margins are low for both designs, although the phase margin for design 2 is very near the 30-60 deg suggested in most textbooks. The gain and phase margins can be included in the structured singular value framework.[16] This was not done here because gain margins and phase margins were not in design specifications. As seen in both designs, gain and phase margins are not necessary for having good parameter margins.

The parameter margin for k for design 2 almost meets the specification 1 for design 1. Although the two designs have very similar lower-parameter margins for k, the controllers achieve this robustness with very different pole and zero locations (see Figs. 5 and 12). Trying to derive similar designs via loop shaping is expected to be quite difficult.

Covering real parameter variations by complex uncertainties was found to be quite conservative. This implies that a controller design procedure that directly takes into account the real nature of k, m_1, and m_2 may give better designs. It is interesting that, even when covering real uncertainties by complex ones in the controller design procedure, the resulting controllers still gave better robustness to real parameter variation than many of the controllers presented at the 1990 and 1991 American Control Conferences.

As a final comment, it should be noted that design specifications must be chosen carefully before the controller is designed. For example, recall that the performance weight w_z was not chosen to have higher gain at low frequency because an impulse disturbance to the mass-spring system gives no steady-state offset. Although the designed controllers will reject impulse disturbances, they give poor rejection of *step* disturbances. If step disturbances are to be expected, then this expectation must be put into the design specifications so that the appropriate weights are chosen in the design procedure. Similar observations can be made concerning sinusoidal disturbances.

VI. Conclusions

Robust controllers were presented for an undamped pair of coupled masses with a noncollocated sensor and actuator. This paper illustrated how to put the system into the structured singular value framework and discussed the strategy for choosing input and output weights. Controllers were designed by D-K iteration, and the resulting high-order controllers were reduced to four states via a Hankel model reduction. The controllers met design specifications such as settling time, actuator constraints, and insensitivity to parameter variation and measurement noise. Time responses were remarkably insensitive to uncertainties in the spring constant. The second design was closed-loop stable with up to 30% independent uncertainty in the parameters.

Acknowledgments

R. Braatz was supported by the Fannie and John Hertz Foundation.

References

[1]Wie, B., and Bernstein, D. S., "Benchmark Problems for Robust Control Design," *Proceedings of the 1990 American Control Conference,* San Diego, CA, 1990, pp. 961-962.

[2]Wie, B., and Bernstein, D. S., "Benchmark Problems for Robust Control Design," *Journal of Guidance, Control, and Dynamics,* Vol. 15, No. 5, 1992, pp. 1057-1059.

[3]Stengal, R., and Marrison, C., "Robustness of Solutions to a Benchmark Control Problem," *Proceedings of the 1991 American Control Conference,* Boston, MA, 1991, pp. 1915-1916.

[4]Balas, G. J., "Robust Control of Flexible Structures: Theory and Experiments," Ph.D. Dissertation, California Institute of Technology, Pasadena, CA, 1990.

[5]Doyle, J. C., "Analysis of Feedback Systems with Structured Uncertainties," *IEE Proceedings Part D,* Vol. 129, 1982, pp. 242–250.

[6]Balas, G. J., Packard, A. K., Doyle, J. C., Glover, K., and Smith, R. S. R., "Development of Advanced Control Design Software for Researchers and Engineers," *Proceedings of the 1991 American Control Conference,* Boston, MA, 1991, pp. 996–1001.

[7]Packard, A. K., "What's New With μ: Structured Uncertainty in Multivariable Control," Ph.D. Dissertation, University of California, Berkeley, CA, 1988.

[8]Glover, K., and Doyle, J. C., "A State Space Approach to H_∞ Optimal Control," *Lecture Notes in Control and Information Sciences: Three Decades of Mathematical Systems Theory: A Collection of Surveys at the Occasion of the 50th Birthday of Jan C. Willems,* edited by H. Nijmeijer and J. M. Schumacher, Vol. 135, Springer-Verlag, New York, 1989.

[9]Glover, K., "All Optimal Hankel-Norm Approximations of Linear Multivariables and Their L^∞-Error Bounds," *International Journal of Control,* Vol. 39, No. 6, 1984, pp. 1115–1193.

[10]Doyle, J. C., *Lecture Notes on Advances in Multivariable Control,* ONR/Honeywell Workshop on Advances in Multivariable Control, Minneapolis, MN, Oct. 1984.

[11]Wedell, E., Chuang, C.-H., and Wie, B., "Stability Robustness Margin Computation for Structured Real-Parameter Perturbations," *Journal of Guidance, Control, and Dynamics,* Vol. 14, No. 3, 1991, pp. 607–614.

[12]Sideris, A., and Pena, R. S., "Fast Computation of the Multivariable Stability Margin for Real Interrelated Uncertain Parameters," *IEEE Transactions on Automatic Control,* Vol. 34, 1989, pp. 1272–1276.

[13]Fan, M. K. H., Tits, A. L., and Doyle, J. C., "Robustness in the Presence of Joint Parametric Uncertainty and Unmodeled Dynamics," *Proceedings of the 1988 American Control Conference,* Atlanta, GA, 1988, pp. 1195–1200.

[14]Young, P. M., and Doyle, J. C., "Computation of the Structured Singular Value with Real and Complex Uncertainties," *Proceedings of the 1990 IEEE Conference on Decision and Control,* Honolulu, HI, 1990, pp. 1230–1235.

[15]Safonov, M. G., "Imaginary-Axis Zeros in Multivariable H_∞-Optimal Control," *Modeling, Robustness and Sensitivity Reduction in Control Systems,* edited by R. F. Curtain, Springer-Verlag, New York, 1987.

[16]Jackson, P., "Applying μ-Synthesis to Missile Autopilot Design," *Proceedings of the 29th IEEE Conference on Decision and Control,* Honoloulu, HI, 1990, pp. 2993–2998.